J. Plasma Fusion Res. SERIES, Vol. 3 (2000) 436–439

Infrared Imaging Bolometry for Long Pulse Discharges on LHD

ASHIKAWA Naoko*, PETERSON Byron J.[1)], WURDEN Glen A.[2)],
SUDO Shigeru[1)] and LHD Experimental groups
Graduate University for Advanced Studies, Toki-shi 509-5292 JAPAN
[1)]National Institute for Fusion Science, Toki-shi 509-5292 JAPAN
[2)]Los Alamos National Laboratory, Los Alamos, NM 87545 USA

(Received: 18 January 2000 / Accepted: 11 April 2000)

Abstract

This diagnostic, known as the segmented mask infrared imaging bolometer (SIB), uses state-of-the-art infrared (IR) imaging technology to measure the temperature rise of each pixel in a two dimensional array mask sandwiching the metal foil. We have designed, constructed, installed and calibrated a version of the SIB for the Large Helical Device (LHD). This diagnostic has a two dimensional view (toroidal and poloidal) of the LHD plasma from an upper port. Through calibration, a representative decay time of $\tau =$ 0.13 sec., and calibration factor of $K = 0.80$ deg./mW were obtained. In addition, we calculate the time varying incident radiation power at the foil using both calibration parameters. In the 3rd cycle of experiments on LHD, we measured the plasma radiation and show the capability of this diagnostic as a steady-state measurement system.

Keywords:
bolometer measurement, infrared camera, plasma radiation

1. Introduction

The various widely used resistive bolometer systems are the standard radiation measurement systems for thermal fusion plasma experiments [1-3]. However, in the case of a future reactor many detectors will be needed, but cables of these resistive bolometers are subject to noise and vacuum leaks at the feedthrough.

The imaging bolometer is a new type of plasma radiation measurement system which uses an infrared (IR) camera [4,5]. We refer to the segmented mask pattern type as the segmented mask infrared imaging bolometer (SIB). In this paper we will report on the first use of an SIB on LHD.

The advantages of an infrared imaging bolometer (IRIB) are as follows: (1) The IR camera is installed outside of the vessel, with no wiring across the vacuum interface. So, this system does not have feedthrough. (2) Change of the IR camera measurement mode depending on the subject of 2-D imaging is very easy i.e. full frame to the line scan mode. (3) 3-D tomography can be achieved using multiple 2-D imaging bolometers.

The first proposal to use an IR camera for a bolometer was by G. Apruzzese and G. Tonini [6] and the segmented mask IR imaging bolometer was proposed [4] and tested on Compact Helical System (CHS) [5]. In this study, about the first steady-state measurement, the IR imaging bolometer is designed, installed and operated on LHD.

*Corresponding author's e-mail: ashikawa@LHD.nifs.ac.jp

2. Design

The system consists of an infrared video camera, a vacuum window, and a reentrant structure that holds a detector mask and pinhole assembly. The present IR camera is an Agema thermovision 900 LW. The spectral response of the Mercury Cadmium Tellride (MCT) detector is 8–12 μm. Stirling cycle cooling is used.

The camera spatial resolution is 272 × 136 pixels at 15 Hz sampling rate, and is reduced to 272 × 68 pixels at 30 Hz. The nominal field of view of the IR camera is 10 × 5 degrees.

The poloidal cross-section of the IRIB design at the LHD 6.5-U port is shown in Fig. 1. In the vacuum vessel the light shield is installed from the inner wall (upper end) to the LHD midplane (lower end). A mask and a pinhole plate are fitted at the lower end. A metal foil is sandwiched between two copper masks, which have a 2-dimensional hole pattern drilled in them. The foil is selected according to the criterion of: (1) low thermal conductivity for high sensitivity, (2) optimization of thickness to keep enough energetic photons, but (3) thin as possible for high sensitivity. We model the mask pixels as solid cylinders, using the differential equation shown in eq. (1).

$$T(r,t)=\frac{2}{b}\times\frac{S_f}{k\times th}\sum_{m=1}^{\infty}\frac{J_0(\beta_m\times r)}{J_1(\beta_m\times b)}\times\frac{1-\exp\left[-\kappa(\beta_m)^2\times t\right]}{(\beta_m)^3}, \quad (1)$$

where k is the thermal conductivity, κ is the thermal diffusivity, S_f is incident power flux, β_m is the m -th J_0 Bessel function roots normalized by the mask pixel radius b [4]. Using this model we adjust the foil radius b and the foil thickness th for various metals to arrive at an optimum set of design parameters in LHD. Using the thermal parameters of different metals, rise time and temperature for various foils are calculated.

We picked the foil material in this case to be aluminum based on its rise time and thermal sensitivity. Additionally, aluminum is available commercially as very thin and large size foils. The resulting foil segments have b = 5.25 mm and th = 0.8 μm, and the total number of pixels on the mask is 118.

The field of view in the poloidal direction of the IRIB as installed in LHD is shown in Fig. 1. The light shielding tube (which prevents stray IR light from other parts of the vessel from coming into the camera field of view) is installed inside the vacuum vessel and this tube has a slit plate installed on the end of the tube on the plasma side and the mask installed inside the tube. The IR vacuum window is installed on the vacuum vessel side of the tube and we use a ZnSe window for the SIB. The IR camera is installed outside vacuum vessel and the view through the ZnSe window is focused on the mask. The plasma radiation is absorbed by the mask foil and the IR camera measures the temperature rise of this heated foil through the ZnSe window. The window transmission is about 95% in the infrared region. The spatial resolution is different in both the poloidal and toroidal directions. In the toroidal direction it is about 17 cm and in the poloidal direction it is about 25 cm at the plasma midplane. This gives a view which is a half field period near the 6.5 port in LHD.

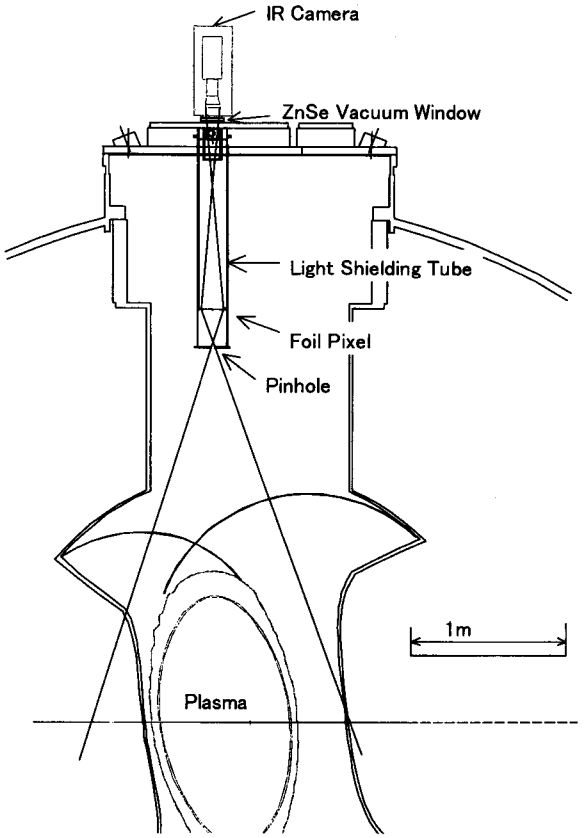

Fig. 1 The IR Imaging Bolometer of field of view on poloidal/radial direction.

3. Calibration

Calibration is necessary because the response of the metal foil surface using the pixel mask is not uniform. This is due to (1) variation in thickness due to manufacturing, (2) the effect of uneven deposition of carbon on the foil and (3) uneven clamping of the foil

between the masks at the pixel edge resulting in an effective radius of the pixel which is larger than the mask pixel size. Each pixel needs to be checked by determining the decay time, τ, and the temperature rise relative to the mask temperature, ΔT due to a unit heat source. The plasma radiation, P_{rad}, can then be calculated as shown in eq. (2)

$$P_{rad} = \frac{1}{K}\left(\Delta T + \tau \frac{\partial T}{\partial t}\right). \qquad (2)$$

Where K is the calibration coefficient. A He-Ne laser is used for this calibration whose power is about 10 mW. τ is decided by the exponential rise time of the foil temperature when a chopper cuts the laser light. K is determined from the temperature rise divided by the incident laser power. To steer the laser light, we used two mirrors and the laser power arriving at the mask is about 80%. The decay time varies from a pixel to a pixel, depending on clamping of the mask and foil, and typically is about 0.13 seconds. The fitting analysis is shown in Fig. 2. In additional, the averaged K is 0.80 deg./mW.

Some of the pixels of the mask have crosstalk with neighboring pixels, in spite of the thick copper mask. Evidently the clamping is imperfect in some spots on the mask (mostly near the edge), causing both the pixel to be effectively larger than the design value, and also causing some thermal leakage. Consequently, we have made a calibration table for each of the 118 pixels.

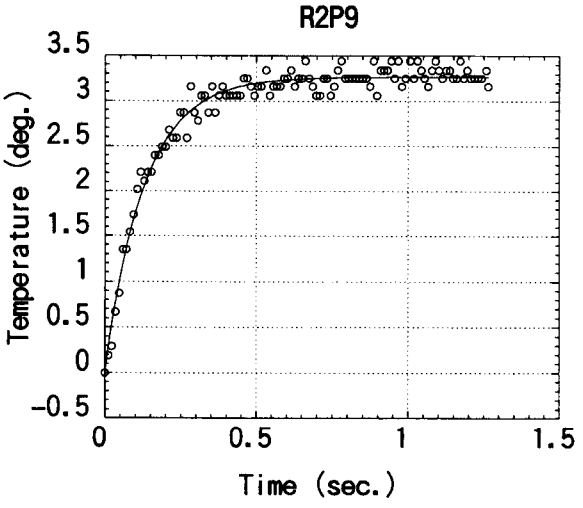

Fig. 2 The fitting analysis for a cooling decay time at a pixel.

Using this calibration data, we can then estimate the incident plasma radiation power at a foil pixel. The radiation power is calculated by eq.(2). dT/dt is estimated using the three point Lagrangian method. The radiation powers on three pixels are shown in Fig. 3(a).

When the plasma discharge is started, the pixels near the mask edge have large signals. Pixel R10P1 decays long after the discharge because clamping of the mask and foil is not good, so the actual pixel area is larger than the mask pixel area and copper masks do not have a strong cooling effect. But later in time, pixel signals fit well compared to the resistive bolometer data. Because the resistive bolometer time resolution is better than the IRIB, fast transient pulse signals can not be detected by the IRIB, but for the total radiation measurement still has sufficient response.

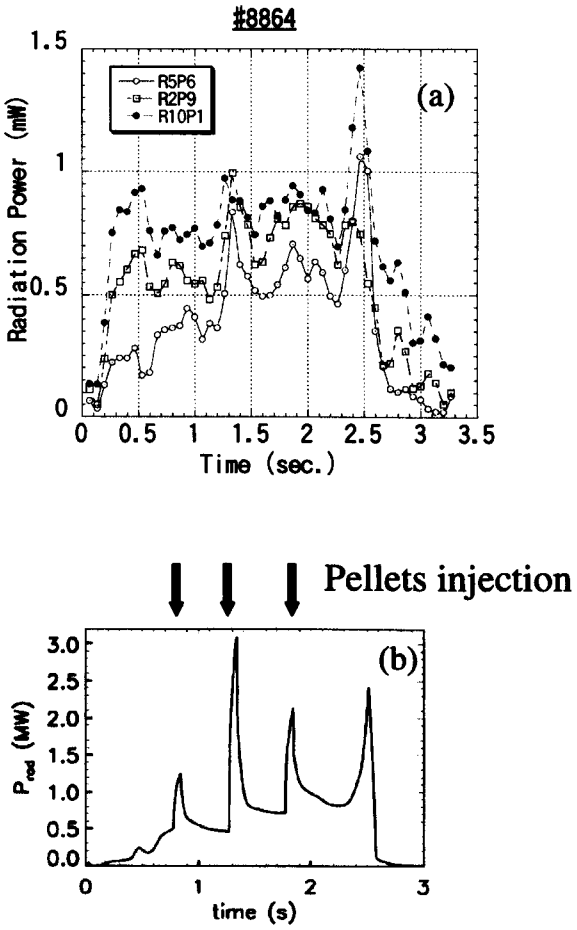

Fig. 3 (a) The incident radiation powers at three different foil pixels as a function of time. (b) The plasma radiation power by the resistive bolometer.

4. The magnetic Field Test of the IR Camera

The present IR camera has several components which might be susceptible to magnetic fields. At a minimum, it has four electric motors. That is a cooling motor, a lens focus motor, and two motors for the x and y scanning mirrors. From our experience, the perturbation on electric motors by the change in LHD magnetic fields is very weak because LHD has a superconducting coil and therefore essentially steady magnetic fields.

We tested the IR camera in a magnetic field below 600 G and have operational conditions of the IR camera as follows:

(1) IR camera was shielded by an iron box with a thickness of th_{box} = 6 mm,
(2) The highest magnetic field outside the iron box is under 400G, as determined by calculations and field measurements,
(3) The optical fiber relay unit (component of the camera) was also installed at a low magnetic field area.

5. Summary

In the LHD 3rd cycle, we have design a segmented mask infrared imaging bolometer system and installed it at 6.5 upper port in LHD. The results are summarized as follows:

(1) We have designed and installed the IR imaging bolometer in LHD, which is the first attempt at a steady-state measurement,
(2) After some problems due to the magnetic field of the superconducting coil were overcome, we acquired a spatial, sequential radiation data for each pixel of the mask,
(3) We have the first plasma data of a steady-state measurement and have demonstrated the capability of this diagnostic as a steady-state measurement system.

The acquisition of data during long plasma shots with the IRIB system is very easy because the storable time duration is dependent only on the hard disk size. We have measured long discharge plasmas up to 70 sec at a 15 Hz sampling rate.

It is has been shown that an IR camera system is very useful, but installation near a fusion reactor operating in steady-state has restrictions caused both by magnetic interference and future nuclear radiation damage issues.

Future work on this technique will automate the application of calibration factors to 2-dimensional array data, and therefore a better understanding of the plasma radiation profile will result when used in conjunction with classical bolometry arrays.

Acknowledgment

This work has been under development through a collaboration between the National Institute for Fusion Science (NIFS)(Japan) and Los Alamos National Laboratory (USA).

References

[1] B.J. Peterson *et al.*, Journal of Plasma and Fusion Research Series (ITC-8), **1**, 382 (1998).
[2] A.W. Leonard, W.H. Meyer, B. Geer, D.M. Behne and D.N. Hill, Rev. Sci. Instrum. **66**, 1201 (1995).
[3] K.F. Mast, H. Krause *et al.*, Rev. Sci. Instrum. **56**, 969 (1985).
[4] G.A. Wurden, B.J. Peterson and S. Sudo, Rev. Sci. Instrum. **68**, 766 (1997).
[5] G.A. Wurden and B.J. Peterson, Rev. Sci. Instrum. **70**, 255 (1999).
[6] G. Apruzzese and G. Tonini, Rev. Sci. Instrum. **61**, 2976 (1990).